Assessment of physical and hydrological properties of biological soil crusts using X-ray microtomography and modeling

Menon, M.; Yuan, Q.; Jia, X.; Dougill, A. J.; Hoon, S. R.; Thomas, Andrew David; Williams, R. A.

Published in:
Journal of Hydrology

DOI:
10.1016/j.jhydrol.2010.11.021

Publication date:
2011

Citation for published version (APA):
Menon, M., Yuan, Q., Jia, X., Dougill, A. J., Hoon, S. R., Thomas, A. D., & Williams, R. A. (2011). Assessment of physical and hydrological properties of biological soil crusts using X-ray microtomography and modeling. *Journal of Hydrology*, *397*(1-2), 47-54. https://doi.org/10.1016/j.jhydrol.2010.11.021

Journal of Hydrology 397 (2011) 47–54

Contents lists available at ScienceDirect

Journal of Hydrology

journal homepage: www.elsevier.com/locate/jhydrol

Assessment of physical and hydrological properties of biological soil crusts using X-ray microtomography and modeling

M. Menon [a,*], Q. Yuan [b], X. Jia [b], A.J. Dougill [a], S.R. Hoon [c], A.D. Thomas [c], R.A. Williams [b]

[a] School of Earth and Environment, University of Leeds, LS2 9JT, UK
[b] School of Process, Environmental and Materials Engineering, University of Leeds, LS2 9JT, UK
[c] Department of Environmental & Geographical Sciences, Manchester Metropolitan University, M1 5GD, UK

ARTICLE INFO

Article history:
Received 17 May 2010
Received in revised form 3 September 2010
Accepted 23 November 2010

This manuscript was handled by L. Charlet, Editor-in-Chief, with the assistance of Ewen Silvester, Associate Editor

Keywords:
Biological crusts
Porosity
Superficial velocity
X-ray microtomography
Lattice Boltzmann
Kalahari soils

SUMMARY

Biological soil crusts (BSCs) are formed by aggregates of soil particles and communities of microbial organisms and are common in all drylands. The role of BSCs on infiltration remains uncertain due to the lack of data on their role in affecting soil physical properties such as porosity and structure. Quantitative assessment of these properties is primarily hindered by the fragile nature of the crusts. Here we show how the use of a combination of non-destructive imaging X-ray microtomography (XMT) and Lattice Boltzmann method (LBM) enables quantification of key soil physical parameters and the modeling of water flow through BSCs samples from Kalahari Sands, Botswana. We quantify porosity and flow changes as a result of mechanical disturbance of such a fragile cyanobacteria-dominated crust. Results show significant variations in porosity between different types of crusts and how they affect the flow and that disturbance of a cyanobacteria-dominated crust results in the breakdown of larger pore spaces and reduces flow rates through the surface layer. We conclude that the XMT–LBM approach is well suited for study of fragile surface crust samples where physical and hydraulic properties cannot be easily quantified using conventional methods.

1. Introduction

Biological soil crusts (BSCs) are formed by an intimate association between soil particles and cyanobacteria, green algae, microfungi, bacteria, lichens and bryophytes which live within or immediately on top of the uppermost millimeters of soil (Belnap and Gardner, 1993). Due to their low moisture requirement and tolerance to extreme temperature and light, they dominate the ground cover in many dryland systems which cover more than one-third of the global land area (Belnap, 2003). For example, in undisturbed areas of Kalahari Sand soils in Botswana, BSCs cover reaches 95% of the soil surface (Dougill and Thomas, 2004). Multiple classification systems are available based on appearance, biomass, and species composition of BSCs (Belnap, 2003). For instance, Thomas and Dougill (2007) used surface characteristics to classify BSCs from Kalahari Sands and linked this to their strength, erosivity and organic carbon content (Berkeley et al., 2005).

BSCs play vital hydrological, geomorphological and ecological roles in drylands (Evans and Johansen, 1999; Viles, 2008). Several studies have demonstrated their roles on controlling soil carbon cycling process including regulation of both photosynthesis activity and soil respiration (Housman et al., 2006; Lange et al., 1998; Thomas and Hoon, 2010), nitrogen fixation (Belnap, 2002; Büdel et al., 2009; Wu et al., 2009), soil aggregation (Belnap, 2006; Zhang et al., 2006), and soil erosion prevention (Belnap, 2006; Eldridge et al., 2000; Ram and Aaron, 2007).

However, the influence of BSCs on hydrological processes such as infiltration remains uncertain and controversial (Belnap, 2006; Evans and Johansen, 1999) due to the lack of measurements of key physical measurements which determine the flow through the surface crust. Warren (2003) analyzed previous studies on infiltration and found that out of 24 field-based studies on infiltration, seven showed that the presence of biological crusts increased infiltration, six showed no effect, and 11 showed decreased infiltration. Warren (2003) concluded that the presence of crusts decreased infiltration as sand content increased (>66%) and increased infiltration as clay contents increased (>15%). However, it is well established that other soil physical properties such as soil structure, porosity and pore characteristics (size, shape, connectivity, tortuosity) significantly influence water flow through soil and these have not been measured in crust hydrology studies to date.

* Corresponding author. Tel.: +44 113 343 1635; fax: +44 113 343 5259.
E-mail addresses: m.menon@leeds.ac.uk (M. Menon), q.yuan@leeds.ac.uk (Q. Yuan), x.jia@leeds.ac.uk (X. Jia), a.j.dougill@leeds.ac.uk (A.J. Dougill), S.Hoon@mmu.ac.uk (S.R. Hoon), A.D.Thomas@mmu.ac.uk (A.D. Thomas), r.a.williams@leeds.ac.uk (R.A. Williams).

0022-1694/$ - see front matter © 2010 Elsevier B.V. All rights reserved.
doi:10.1016/j.jhydrol.2010.11.021

Data on these underlying soil physical parameters would form a stronger physical basis and help interpret the infiltration data and ascertain the role of BSCs on crusts on infiltration (Belnap, 2006). However, measurement of structure or porosity without disturbance to the crusts is a methodological challenge, especially when dealing with fragile samples like BSCs.

In addition to porosity and pore characteristics, infiltration or run off are also affected by several other properties of the BSCs such as pore clogging or hydrophobicity, depending on the type and the amount of organisms in the crust (Belnap 2006). Most organisms have the ability to swell upon wetting contributing to hydrophobicity and the clogging of soil pores (Verrecchia et al., 1995; Kidron et al., 1999). Similarly, when BSCs are disturbed mechanically, infiltration can be significantly affected (Eldridge et al., 2000) due to the changes in structure, porosity and pore characteristics. The effect depends fundamentally on the type of crust, the amount of force applied and initial moisture conditions. The effect of mechanical disturbance on infiltration can be only explained with the help of porosity or bulk density changes before and after the application of force and as yet no studies quantify the impact of mechanical disturbance on structure and porosity of fragile dryland soil crusts.

In order to establish the influence of BSCs on infiltration, we need to develop and apply non-destructive quantification of porosity and structure and an independent assessment of flow which is based on key soil physical properties and not affected by field disturbance or properties of crusts such as hydrophobicity or pore clogging. Given this, we formulated the following objectives for this study:

(1) to quantify and assess porosity and structure of different types of BSC from a study site in the Kalahari using non-destructive X-ray microtomography (XMT) and the modeling of flow using Lattice Boltzmann method (LBM) and
(2) to assess the impact of mechanical disturbance (vertical impact) on the porosity of, and flow through, a cyanobacteria-dominated BSC.

2. Methods

2.1. Sample collection and preparation

BSC samples were collected from a southern Kalahari location near Tsabong (26°3'S–22°27'E), Botswana where a series of ongoing studies are assessing the biological and biogeochemical make up of crusts (Berkeley et al., 2005; Thomas and Dougill, 2007; Mager, 2010; Thomas and Hoon, 2010). Kalahari sand soils are typically 96–98% fine sand and are found across an area of over 2 million km^2 of southern Africa (Wang et al., 2007). The mean annual rainfall of the study site is *c.* 320 mm. The BSCs of Kalahari are classified into three types based on their form and morphology (Dougill and Thomas, 2004), as represented in Fig. 1. Type 1 BSCs represent the early stage of crust formation indicated by a delicate and thin layer of aggregated sand materials on the surface, often buried under aeolian deposits with no distinct colouration. Type 2 crusts are a few millimeters thick with speckles of colouration, whereas Type 3 crusts are dark brown or black in colour with a clear surface microtopography. Both Types 1 and 2 are cyanobacteria-dominated whereas Type 3 crusts are made up of both cyanobacteria and surface lichen communities (Thomas and Dougill, 2007). The order of their fragility (measured in terms of crust strength with a portable needle penetrometer) is Type 1 > Type 2 > Type 3 and the reverse order is true for their structural development and surface microtopography/roughness (see Thomas and Dougill, 2007). Intact soil cores and crust samples were collected in small petri dishes and wrapped in cotton. Cyanobacterial

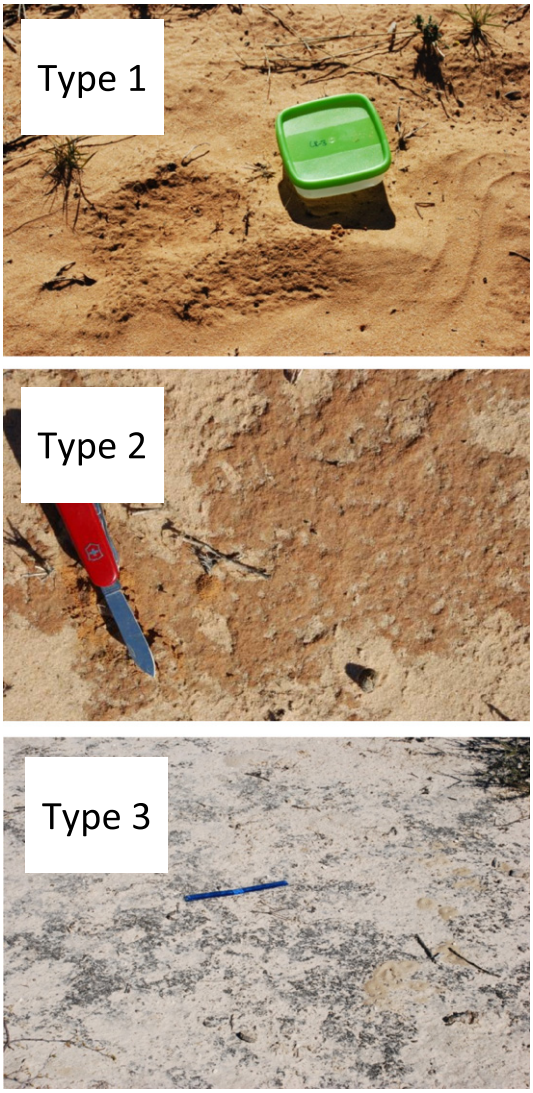

Fig. 1. Photographs showing various crusts Types (1–3) found in Kalahari. The order of their fragility is Type1 > Type2 > Type3. The Types 2 and 3 were used for this study.

Type 2 and mixed cyanobacteria–lichenous Type 3 samples were able to be packed and transported to the laboratory without breaking up and as such were used for this study. Type 1s (early development-stage cyanobacterial crusts) were not studied due to their very low compressive strength, making intact transit to a distant imaging facility was difficult to ensure.

2.2. XMT imaging

X-ray microtomography (XMT) is a non-destructive 3D imaging technique widely used for visualization and quantification of inner structure (for soil applications see review by Taina et al., 2008) without tedious sample preparation. The high resolution images obtained using XMT typically show spatial arrangement (structure) of solid particles and pores in space. The facility consists of an X-ray source, a detector and the sample in between. The XMT scanner (Phoenix Nanotom 160 NF) used for this study has a nano-focus X-ray tube, capable of producing a spot-size (akin to aperture in pin-hole imaging) of less than 1 μm, up to 180 kV tube voltage and 880 μA tube current, giving a 15 W power output. Detail detectability can go down to 200–300 nm. The CCD X-ray detector array has 2304 × 2304 pixels.

Given a fixed X-ray detector size, image resolution is inversely proportional to the sample size used. Therefore, we used a small piece of crust (approximately 5 mm diameter) in order to achieve a resolution of 2–3 μm and to study the crust micro-structure and to model water flow. We scanned two Type 2 samples and one Type 3 sample. We chose one Type 2 sample to study the influence of mechanical disturbance on soil structure and permeability. To apply disturbance, the sample was vertically arranged in a plastic sample holder, with the surface layer at the top. A force was applied by dropping a weight of 200 g from a distance of 1 cm to simulate the impact of trampling. The sample was imaged before and after disturbance to study porosity and structural changes directly.

The scan data was imported using *DigiUtility* – an in-house code for processing and visualizing volumetric datasets. For the simulations reported here, it was used for cutting out a sub-section from the full scan volume, scaling down the resolution, saving it in a format recognisable by the LBM code.

In order to understand pore size distribution of the 3D volumes, we also calculated mean empty space (MES), which is a size measure of the pore space. This was done by picking at random a pore (empty) site and measure from this point the dimensions of the pore space along *X*, *Y* and *Z* axes. The procedure is repeated for a large number (65,500) of random points and the averages are taken.

Table 1
Model parameters and their description with units.

Parameter type with units	Value
f (pressure gradient)	0.001
τ (relaxation number)	1
ν_{phys} (kinematic viscosity of water), [$m^2\ s^{-1}$]	1×10^{-6}
β (resolution) [pixels per meter]	1×10^5

2.3. LBM modeling

The Lattice Boltzmann method (LBM) offers numerical solutions for simulating flow in and through complex porous media using high resolution 3D structure obtained via XMT (Succi, 2001; Sukop and Thorne, 2006). LBM offers quantification and visualization of superficial velocity (equivalent to Darcy hydraulic conductivity) based on the porosity and pore characteristics. The advantages of LBM over conventional computational fluid dynamics (CFD) approaches are mainly its simplicity, the possibility to use larger datasets or images of complex geometry, and its speed (particularly when the meshing requirement of conventional CFD approaches is taken into account). A detailed description of the method can be found in monographs elsewhere (Succi, 2001; Sukop and Thorne, 2006; Wolf-Gladrow, 2000) together with its capability to model permeability through porous media obtained using XMT (Selomulya et al., 2006; Videla et al., 2008; Zhang et al., 2005).

All inputs and outputs to LBM are customarily in lattice units. For length scale, one lattice unit is the linear size of one grid cell (lu); for time, it is one time step (ts). Both are set to have a nominal value of 1. Velocity is given in units of lu ts^{-1}, and kinematic viscosity in $lu^2\ ts^{-1}$. To convert superficial velocity U from lattice units to physical ones, it is assumed that the value of the Reynolds number, $\mathrm{Re} = \frac{UL}{\nu}$, remain the same in both lattice and physical worlds, thus

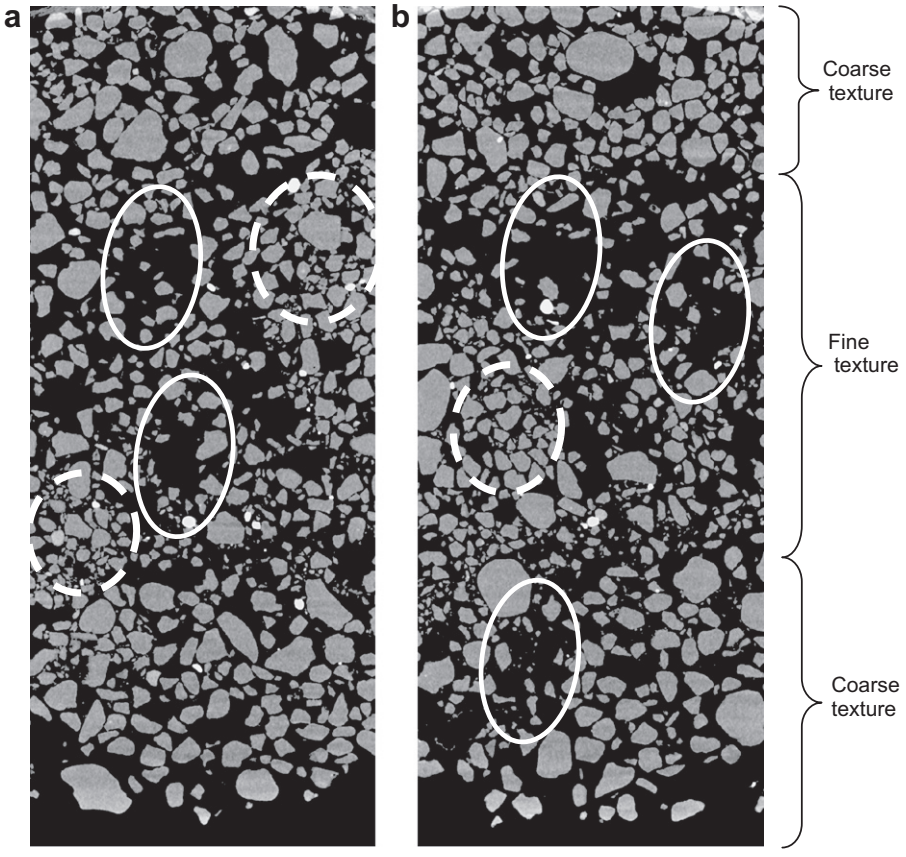

Fig. 2. (a and b) Two examples of 2D cross-sections of Type 2 crusts with 3 μm resolution (image dimensions: 6576 × 2700 μm). The white ellipses in the left image show large voids in the structure and the dotted white circle shows the aggregation. The sample was clearly showing texture variations within the sample, i.e. a fine textured sand is sandwiched between two coarse sand grains.

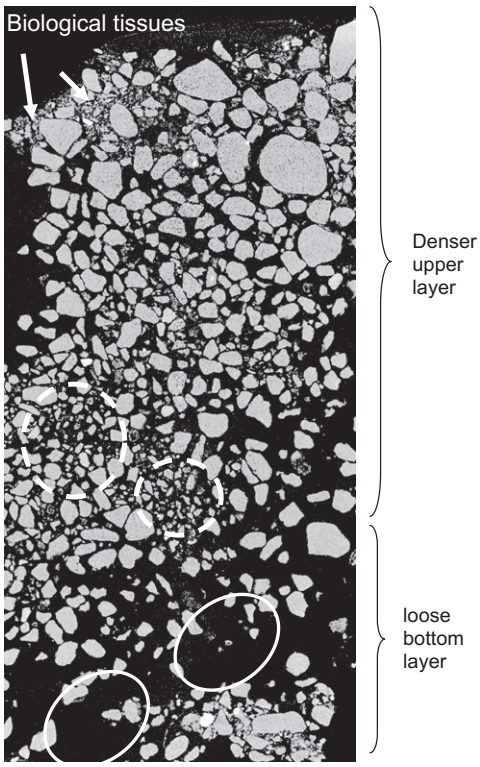

Fig. 3. An example 2D view of Type 3 crusts with 3 μm resolution (image dimensions: 5805 × 2700 μm) with denser layer at the top with a loose structure at the bottom. The biological tissues were seen at the top of the crusts. Aggregated regions (dotted circles) are clearly visible.

$$U_{phys} = \frac{\nu_{phys}}{L_{phys}} \mathrm{Re}_{lattice} = \frac{\nu_{phys}}{L_{phys}} \frac{U_{lattice} L_{lattice}}{\nu_{lattice}} = \frac{6\nu_{phys} U_{lattice} \beta}{2\tau - 1} \quad (1)$$

where L is a characteristic length, τ a relaxation parameter used as input to LBM, ν kinematic viscosity of fluid (water), and β resolution given in pixels per meter. Values of these parameters and of the LBM calculated superficial velocity are summarised in Table 1. The final superficial velocity in physical units is equivalent to Darcy hydraulic conductivity. We use the superficial velocity throughout this paper.

2.4. Porosity measurement of BSCs using stereopycnometer

In order to compare the porosity obtained from XMT with more conventional approaches, we also measured porosity in an engineering soils laboratory using a Helium gas Quantachrome stereopycnometer (model SPY-2) to determine porosity of BSCs (Lowell et al., 2004).

3. Results

In this section, we present the images obtained on BSC Types structure using the XMT method including pre– and post-disturbed samples, followed by results from LBM simulations comparing both the two types of crust sampled and also the impacts of disturbance on the cyanobacterial crust.

3.1. Micro-structural features of the crusts

Figs. 2 and 3 show example cross-sectional slices gained through XMT scanned 3D crust structures. Several hundreds of these 'digital' slices can be made in any direction (*XY* or *XZ* or *YZ*)

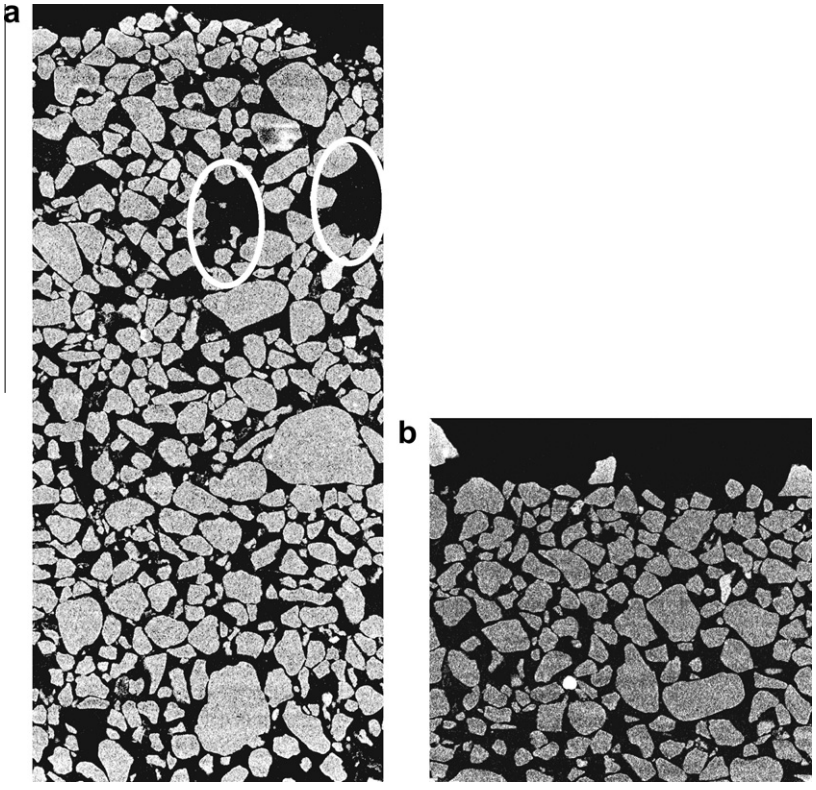

Fig. 4. (a and b) Images showing Type 2 crust with 2 μm resolution before (a) and after (b) a simulated mechanical impact, the dimensions of the sample prior to the impact was 3978 × 1800 μm (a) and after the impact was 1906 × 2008 μm (b). The mechanical impact has significantly compacted the samples (approximately 50% reduction in the length). Most of the large voids (ellipses) found in prior to the disturbance were almost disappeared after the mechanical impact, reducing the total porosity.

to virtually navigate through the sample to enable improved understanding and quantification of the inner structure. The slices shown here are from middle part of the crust sample. The grey objects in Figs. 2 and 3 represent sand particles and black indicates voids. These images show the presence of macropores (solid ellipses) and aggregation (dashed circles) revealing the important micro-scale soil structural heterogeneity within crusts examples of which are highlighted in the figures. The particle size distribution within cyanobacterial Type 2 crusts (Fig. 2) shows that fine textured sand grains are typically sandwiched between coarse textured grains. Many macropores appear long and continuous which will significantly influence the flow through the crusted layer. Clusters of sand grains/aggregates are also visible in many parts of the samples which are most likely due to the aggregation effects caused by sticky extracellular polysaccharide compounds produced by BSCs (Mager, 2010) as illustrated in earlier publications using electron microscopy (see Belnap, 2006; Zhang et al., 2006).

The presence of additional biological tissues (notably lichens), especially on the upper part of the sample, can be clearly seen in the images of the Type 3 crust (Fig. 3). Type 3 crust revealed a much more compacted top layer with a relatively loose bottom layer. Example images (such as in Fig. 3) showed large voids in the samples, typically towards the middle to bottom part of the sample.

Fig. 4a shows the second sample of cyanobacterial Type 2 sample prior to the mechanical impact. Both samples (Figs. 2 and 4a) fall under same Type of crusts, yet differ significantly in their structure. For example, the first sample (Fig. 2a and b) showed several macropores and channels, whereas the second sample a few macropores (Fig. 4a). Fig. 4b shows the crust after the mechanical impact. Macropores are visible prior to the impact (Fig. 4a), but disappeared after the mechanical impact. The vertical disturbance significantly reduced the crust dimensions (compaction) and resulted in a more uniform packing of sand grains.

3.2. LBM simulation

We modeled flow using 3D BSC structures obtained (including the post-disturbed sample) via XMT. The XMT datasets, which originally had 3 μm per voxel (volumetric pixel) resolution, were scaled down to 10 μm per voxel to enable a larger (and more representative) sample volume to fit in the available RAM for LBM simulations. For simulations, top denser parts of crusts were chosen.

The flow in the simulation is from the crust surface down so as to simulate the infiltration process. Fig. 5 shows examples of cross-sectional views of the LBM simulated velocity distribution in Types 2 and 3 crusts respectively. Warm colours indicate higher

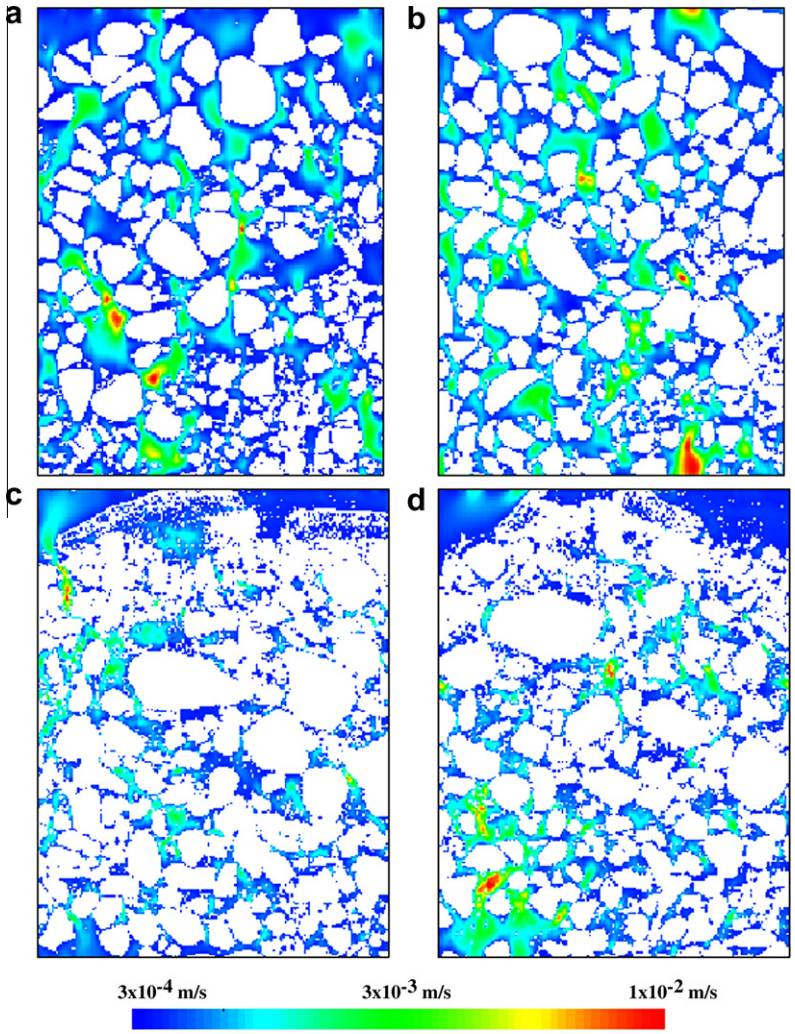

Fig. 5. Flow rate distributions of Type 2 (a and b) and Type 3 (c and d), simulated using LBM (DigiFlow). Solid phase (sand particles and tissues) areas are given as white. Warm colours represent areas with relatively higher flow rates. Due to the large voids and channels in the structure of Type 2, more flow strands (green and red colours) could be observed. The sample size is 2500 × 1800 μm.

superficial velocity. Figures illustrate how structure and porosity is influenced by structure porosity of the medium. Similarly, Fig. 6 shows the flow distribution in 3D in two examples slices of cyanobacterial Type 2 crusts before (a) and after (b) the disturbance. The number of flow strands was significantly fewer prior to the disturbance of crusts compared to post-disturbance as mechanical disturbance increased the number of flow strands, resulting in a more uniform flow pattern.

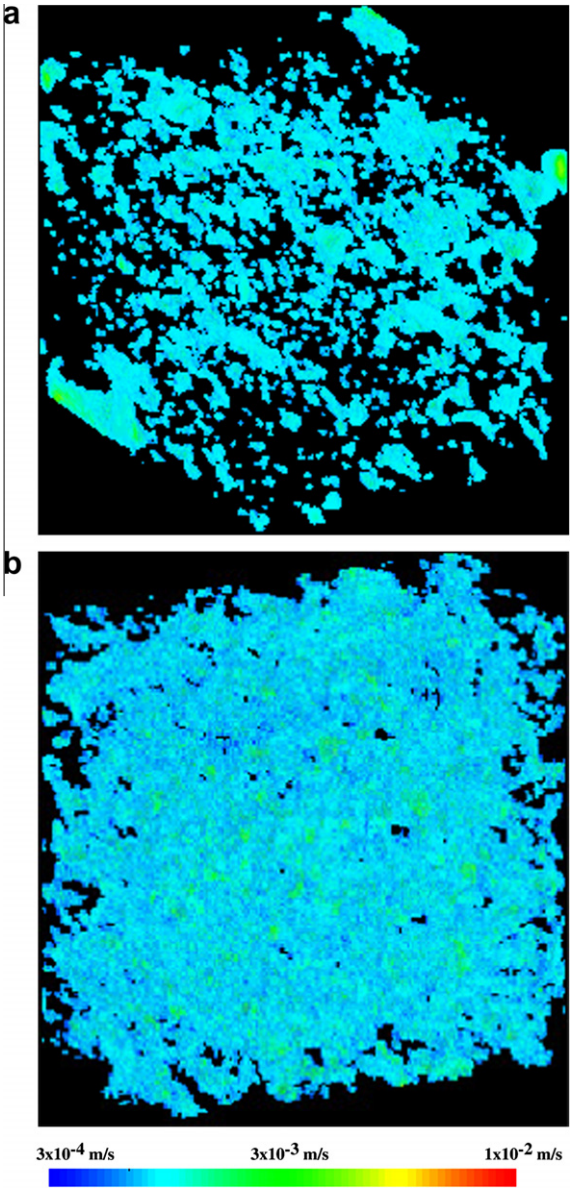

Fig. 6. (a and b) Flow rate distributions in three dimensions of a fragile cyanobacterial dominant crust before (a) and after (b) disturbance in 3D. The colours represent flow strands in 3D in the solid volume (black). Prior to the impact, the flow was confined to a few pores (a). Mechanical disturbance disrupted the existing flow strands and pores to numerous finer ones, subsequently reducing the superficial velocity of the crust (b). The sample sizes were 2500 × 1800 × 1800 μm for (a), 960 × 1800 × 1800 μm for (b).

LBM simulated superficial velocity is given in Table 2 along with porosity (by volume) obtained by XMT. The superficial velocity is the function of porosity. Even within the same type of crust a significant variation in porosity was found (Type 2 samples 1 and 2). Comparing the reduction of porosity and superficial velocity of pre and post-disturbed samples it was found that the mechanical impact has caused a reduction of *c.* 10% in the total porosity resulting in 36% reduction in superficial velocity. The porosity of the Type 3 crust was thus comparable to the post-disturbed Type 2 sample (Table 2).

3.3. Porosity and pore size distribution

The porosity of Types 2 and 3 samples measured in the laboratory using stereo pycnometer were 32.39 ± 3.28% (mean ± standard error) and 35.02 ± 5.24% by volume, respectively. The measurements were in good agreement with the porosity of most samples obtained via XMT.

Table 2 shows the pore size distribution (micro, meso and macro pores) based on MES calculations from each crust type. Type 2 sample 1 had the highest proportion (95%) of macropores among all samples. The pore size distribution of Type 3 sample was in between two Type 2 samples. As a result of mechanical impact, marginal increase in mesopores (3%) was observed.

4. Discussion

This study provides a first quantitative micro-scale assessment of how dryland BSCs influence soil physical properties such as porosity, structure and water flow by using the non-invasive imaging and modeling of different soil crust types and assessment of the impacts of disturbance of a crust. Previously using scanning electron microscopy (SEM), researchers have published images (2D) of BSCs (e.g. Belnap 2006; Zhang et al., 2006; Thomas and Dougill, 2007) to show aggregation of sand particles by sticky extracellular polysaccharides secreted by crust organisms. The XMT method used here enables the further study of the interior structure and rapid quantification of porosity for BSCs and will enable more detailed experiments to be designed to examine the controls that crusts exert on surface infiltration across the worlds drylands.

The XMT images showed micro-scale heterogeneity in the distribution of sand particles and of pores in BSCs. The total porosity and pore sizes were quantified using image analysis tools on a volume basis and showed heterogeneity within the same Type of crust (Type 2 – cyanobateria-dominated crusts). XMT measurements also showed that porosity of Type 3 (lichen-dominated crust) samples was lower than cyanobacteria-dominated Type 2 crusts. The difference is most likely due to the presence of the lichenous tissues within the better developed crusts. The porosity measurements of samples were in good agreement with porosity measured in the laboratory using a stereo pycnometer. Porosity of unconsolidated Kalahari Sand can be as high as 49% (Wang et al., 2007) and most of the crust samples analyzed (using XMT

Table 2
The porosity (%), pore size fractions (%) and superficial velocity of BSCs obtained from XMT digital images and LBM simulations.

Type of crust	Sample size (μm)	Total porosity (vol.%)	Pore size fractions (%)			Superficial velocity	
			⩽30 μm	30–50 μm	⩾50 μm	$U_{lattice}$	U_{phys} (ms^{-1})
Type 2 sample 1	2500 × 1800 × 1800	47.4	2	3	95	2.19×10^{-3}	1.31×10^{-3}
Type 2 sample 2	2500 × 1800 × 1800	34.1	11	12	76	5.34×10^{-4}	3.20×10^{-4}
Type 3 sample 1	2500 × 1800 × 1800	30.9	9	10	81	3.41×10^{-4}	2.05×10^{-4}
Type 2 sample 2 (post-disturbed)	960 × 1800 × 1800	30.4	10	14	76	3.40×10^{-4}	2.04×10^{-4}

or stereopynometer) had far lower porosity than this, indicating the impact of crust in reducing total porosity.

Images presented here also showed that crust structure varies significantly within and between the samples. The internal structure of crust is known to be influenced by the amount and type of micro-organisms in crusts which typically shows a high degree of spatial heterogeneity (Belnap, 2006).

Another significant advance provided by this study is the application of LBM to predict flow of BSCs based on 3D physical structure including the links between physical and hydraulic properties. LBM provides an opportunity to visualize the flow distribution (Fig. 5), where difference in the flow rates can be found within the same sample. The results (Table 2) show how the structure and porosity influence water flow patterns in different BSCs. Within the same Type 2 cyanobacteria-dominated crusts, we observed an order of magnitude difference in superficial velocity between the two samples, primarily due to the large difference in the total porosity and the pore size distribution (Table 2).

Field studies from the same location using a double ring infiltrometer show that hydraulic conductivity of cyanobacteria (Type 2) crusts were an order of magnitude higher (10^{-4} ms^{-1}) than better developed and lichenous Type 3 (10^{-5} ms^{-1}). Similar order of magnitude and trends were also observed by Veste et al. (2001) for cyanobacterial crust dominated crusts and the lichen-dominated crusts of the Negev, Israel. The lack of *in situ* soil physical measurements in previous studies impose difficulties in how to interpret and compare with our results, although trends in superficial velocity and hydraulic conductivity measurements are broadly comparable with cyanobacteria-dominated crusts being more permeable than lichen-dominated crusts.

The difference between the simulated superficial velocities and field experiments is also contributed by some properties of the crusts such as hydrophobicity, surface sealing and clogging of pores upon wetting as a result of swelling and expansion of biomass within BSCs (Campbell, 1979; Eldridge and Greene, 1994; Verrecchia et al., 1995; Kidron et al., 1999). This is especially true for lichen-dominated crusts. These properties significantly contribute to the underestimation of the infiltration rates for better developed lichenous crusts.

For the first time, we also quantified the impact of disturbance on porosity and flow patterns of a cyanobacterial soil crust. XMT–LBM approaches demonstrated (Figs. 4 and 6) the changes in the porosity and flow patterns in pre- and post-disturbed crusts. At the micro-scale, a force applied on the crust in the vertical direction significantly reduces the modeled flow rate. The large voids (Figs. 4a and b) and channels diminished and flow strands were uniformly distributed after disturbance, which resulted in a greater reduction in the superficial velocity in the post-disturbed sample. Experiments conducted in the field conditions with simulated disturbance on Type 2 crusted surfaces also showed similar trend, i.e. a decrease in hydraulic conductivity as a result of disturbance. The modeled results are also in good agreement with field measurements of infiltration rates for Kalahari sand soils (Dougill et al., 1998).

5. Assessment of the XMT–LBM approach

For fragile soil surface samples such as BSCs, the combination of XMT and LBM provides a non-destructive, faster and, most importantly, robust approach that allows the micro-structure of soil crusts to be visualized. The XMT was particularly successful to image 'the whole structure' of crusts. XMT images can be used for visualization and quantification of porosity as well, without cumbersome sample preparation. LBM was found particularly useful to simulate the flow using 3D structure. This study also illustrated the possibility to use these methods to study structural changes as demonstrated by our simulated mechanical impact study on cyanobacterial Type 2 crusts. Most available methods do not allow a pre and post-assessment of structure using visualization and quantification at the same time. Another use of LBM results is the visualization and characterization of flow pathways. As illustrated in Fig. 5, similar-sized pores that appear in a cross-section do not necessarily make similar contribution to flow resistance.

XMT facilities are expensive and not as accessible as other (more conventional) measurement facilities, which limits the number of samples can be studied. Given the small sample size, for the results to be truly representative, it may be necessary to analyze several samples using XMT to be able to examine spatial variability between and within Types of crusts across dryland regions.

6. Conclusions

This study has demonstrated the use of XMT and LBM to overcome one of the major methodological constraints to study physical and hydrologic properties of fragile BSCs that cover much of the worlds dryland soil surface. Using these methods, we were able to interpret flow characteristics based on physical properties. XMT yields high resolution images of various crusts types, which is useful to quantify porosity and understand innate structure of these crusts. We have also demonstrated how mechanical impact could affect the crust porosity and flow in this paper. For the future, we need more comprehensive studies in order to account the heterogeneity of samples.

Acknowledgements

The authors are thankful to Ms. Alice Johnston, Manchester Metropolitan University, UK for field infiltration data and Mr. Carlos Grattoni, School of Earth and Environment, University of Leeds, UK for helping with laboratory soil physical measurements. The research was conducted under the auspices of a Government of Botswana Research Permit Number EWT8/36/4 VIII(4) and linked to a University of Leeds Research Fellowship held by Manoj Menon.

References

Belnap, J., 2002. Nitrogen fixation in biological soil crusts from southeast Utah, USA. Biology and Fertility of Soils 35 (2), 128–135.

Belnap, J., 2003. Microbes and microfauna associated with biological soil crusts. In: Belnap, J., Lange, O.L. (Eds.), Biological Soil Crusts: Structure, Function, and Management. Berlin, Springer-Verlag, pp. 167–174.

Belnap, J., 2006. The potential roles of biological soil crusts in dryland hydrologic cycles. Hydrological Processes 20 (15), 3159–3178.

Belnap, J., Gardner, J.S., 1993. Soil microstructure in soils of the Colorado plateau – the role of the cyanobacterium *Microcoleus vaginatus*. Great Basin Naturalist 53 (1), 40–47.

Berkeley, A., Thomas, A.D., Dougill, A.J., 2005. Spatial dynamics of biological soil crusts: bush canopies, litter and burial in Kalahari rangelands. African Journal of Ecology 43, 137–145.

Büdel, B., Darienko, T., Deutschewitz, K., Dojani, S., Friedl, T., Mohr, K.I., Salisch, M., Reisser, W., Weber, B., 2009. Southern African biological soil crusts are ubiquitous and highly diverse in drylands, being restricted by rainfall frequency. Microbial Ecology 57 (2), 229–247.

Campbell, S.E., 1979. Soil stabilization by a prokaryotic desert crust: implications for Precambrian land biota. Origins of Life and Evolution of Biospheres 9, 335–348.

Dougill, A.J., Thomas, A.D., 2004. Kalahari sand soils: spatial heterogeneity, biological soil crusts and land degradation. Land Degradation and Development 15 (3), 233–242.

Dougill, A.J., Heathwaite, A.L., Thomas, D.S.G., 1998. Soil water movement and nutrient cycling in semi-arid rangeland: vegetation change and system resilience. Hydrological Processes 12, 443–459.

Evans, R.D., Johansen, J.R., 1999. Microbiotic crusts and ecosystem processes. Critical Reviews in Plant Sciences 18 (2), 183–225.

Eldridge, D.J., Greene, R.S.B., 1994. Assessment of sediment yield by splash erosion on a semi-arid soil with varying cryptogam cover. Journal of Arid Environments 26, 221–232.

Eldridge, D.J., Zaady, E., Shachak, M., 2000. Infiltration through three contrasting biological soil crusts in patterned landscapes in the Negev, Israel. Catena 40 (3), 323–336.

Housman, D.C., Powers, H.H., Collins, A.D., Belnap, J., 2006. Carbon and nitrogen fixation differ between successional stages of biological soil crusts in the Colorado Plateau and Chihuahuan Desert. Journal of Arid Environments 66 (4), 620–634.

Kidron, G.J., Yaalon, D.H., Vonshak, A., 1999. Two causes for runoff initiation on microbiotic crusts: hydrophobicity and pore clogging. Soil Science 164 (1), 18–27.

Lange, O.L., Belnap, J., Reichenberger, H., 1998. Photosynthesis of the cyanobacterial soil-crust lichen Collema tenax from arid lands in southern Utah, USA: role of water content on light and temperature responses of CO_2 exchange. Functional Ecology 12, 195–202.

Lowell, S., Shields, J.E., Thomas, M.A., Thommes, M., 2004. Characterization of Porous Solids and Powders: Surface Area, Pore Size and Density. Springer, Netherlands.

Mager, D.M., 2010. Carbohydrates in cyanobacterial soil crusts as a source of carbon in the southwest Kalahari, Botswana. Soil Biology and Biochemistry 42 (2), 313–318.

Ram, A., Aaron, Y., 2007. Negative and positive effects of topsoil biological crusts on water availability along a rainfall gradient in a sandy and area. Catena 70 (3), 437–442.

Selomulya, C., Tran, T.M., Jia, X., Williams, R.A., 2006. An integrated methodology to evaluate permeability based on measured microstructures. AIChE Journal 52, 3394–3400.

Succi, S., 2001. The Lattice Boltzmann Equation for Fluid Dynamics and Beyond. Oxford Science Publications, Oxford.

Sukop, M.C., Thorne Jr., D.T., 2006. Lattice Boltzmann Modeling: An Introduction for Geoscientists and Engineers. Springer-Verlag, Berlin.

Taina, I.A., Heck, R.J., Elliot, T.R., 2008. Applications of X-ray computed tomography to soil science: a literature review. Canadian Journal of Soil Science 88, 1–20.

Thomas, A.D., Dougill, A.J., 2007. Spatial and temporal distribution of cyanobacterial soil crusts in the Kalahari: implications for soil surface properties. Geomorphology 85 (1–2), 17–29.

Thomas, A.D., Hoon, S.R., 2010. Simulated rainfall pulses and carbon dioxide fluxes from Kalahari Sands. Journal of Arid Environments 74, 131–139.

Veste, M., Littmann, T., Breckle, S.-W., Yair, A., 2001. The role of biological soil crusts on desert sand dunes in the northwestern Negev, Israel. In: Breckle, S.-W., Veste, M., Wucherer, W. (Eds.), Sustainable Land Use in Deserts. Springer, Berlin, pp. 357–367.

Verrecchia, E., Yair, A., Kidron, G.J., Verrecchia, K., 1995. Physical-properties of the psammophile cryptogamic crust and their consequences to the water regime of sandy soils, north-western Negev desert, Israel. Journal of Arid Environments 29, 427–437.

Videla, A.R., Lin, C.L., Miller, J.D., 2008. Simulation of saturated fluid flow in packed particle beds – the Lattice-Boltzmann method for the calculation of permeability from XMT images. Journal of the Chinese Institute of Chemical Engineers 39, 117–128.

Viles, H.A., 2008. Understanding dryland landscape dynamics: do biological crusts hold the key? Geography Compass 2 (3), 899–919.

Wang, L., D'Odorico, P., Ringrose, S., Coetzeec, S., Macko, S.A., 2007. Biogeochemistry of Kalahari sands. Journal of Arid Environments 71, 259–279.

Warren, S.D., 2003. Synopsis: influence of biological soil crusts on arid land hydrology and soil stability. In: Belnap, J., Lange, O.L. (Eds.), Biological Soil Crusts: Structure, Function, and Management. Springer-Verlag, Berlin, pp. 349–360.

Wolf-Gladrow, D.A., 2000. Lattice-Gas Cellular Automata and Lattice Boltzmann Models. Springer-Verlag, Berlin.

Wu, N., Zhang, Y.M., Downing, A., 2009. Comparative study of nitrogenase activity in different types of biological soil crusts in the Gurbantunggut Desert, Northwestern China. Journal of Arid Environments 73 (9), 828–833.

Zhang, X., Deeks, L.K., Bengough, A.G., Crawforda, J.W., Young, I.M., 2005. Determination of soil hydraulic conductivity with the Lattice Boltzmann method and soil thin-section technique. Journal of Hydrology 306, 59–70.

Zhang, Y.M., Wang, H.L., Wang, X.Q., Yang, W.K., Zhang, D.Y., 2006. The microstructure of microbiotic crust and its influence on wind erosion for a sandy soil surface in the Gurbantunggut Desert of Northwestern China. Geoderma 132 (3–4), 441–449.